Surface Structures and Properties of Polystyrene/Poly(methyl methacrylate) Blends and Copolymers

William C. Johnson, Jie Wang, and Zhan Chen*

Department of Chemistry, University of Michigan, Ann Arbor, Michigan 48109

Received: September 24, 2004; In Final Form: January 31, 2005

Sum frequency generation (SFG) vibrational spectroscopy has been applied to study the molecular surface structures of polystyrene (PS)/poly(methyl methacrylate) (PMMA) blends and the copolymer between PS and PMMA (PS-*co*-PMMA) in air, supplemented by atomic force microscopy (AFM) and contact angle goniometer. Both the blend and the copolymer have equal weight amounts of the two components. SFG results show that both components, PS and PMMA, can segregate to the surface of the blend and the copolymer before annealing, although PMMA has a slightly higher surface tension. Upon annealing both SFG results and contact angle measurements indicate that the PS segregates to the surface of the PS/PMMA blend more but no change occurs on the PS-*co*-PMMA surface. AFM images show that the copolymer surface is flat but the 1:1 PS/PMMA blend has a rougher surface with island like domains present. The annealing effect on the blend surface morphology has also been investigated. We collected amide SFG signals from interfacial fibrinogen molecules at the copolymer or blend/protein solution interfaces as a function of time. Different time-dependent SFG signal changes have been observed, showing that different surfaces of the blend and the copolymer mediate fibrinogen adsorption behavior differently.

1. Introduction

Because of their excellent surface properties, polymer materials have been extensively used as biomedical implants, biosensor materials, adhesives, lubricants, and corrosion resistance materials.[1−7] Polymer blends and copolymers provide ways to control the characteristics of a single polymer material by combining the properties of individual polymers. They are important polymer materials because their surface structures and properties may be different from those in the bulk, resulting in materials with both required surface and bulk properties.[1−7] Studies have revealed that in a polymer blend or a copolymer the lowest surface free energy component will be enriched at the polymer surface in order to minimize the free energy of the entire system.[8−10] By variation of the bulk concentration of the components, surface structures and properties of polymer blends and copolymers can be varied stepwise.[11]

Polymer blend surfaces have been characterized by a wide range of surface sensitive methods such as X-ray photoelectron spectroscopy (XPS),[12−15] secondary ion mass spectrometry (SIMS),[15−17] atomic force microscopy (AFM),[14,15,18−26] neutron reflectivity,[27,28] and contact angle goniometry.[29,30] XPS and SIMS have been used to study the surface composition of polymer blends.[12−17,31] However, both of them require high vacuum to operate and cannot be applied to study surface structures of polymer materials in other chemical environments, e.g., in air or in liquids. Contact angle goniometry is used to study the surface tension or surface energy,[30] but it cannot provide chemical information on surfaces. AFM is an effective probe for measuring the properties of the surface such as morphology, adhesion, and friction in air and in liquids with excellent spatial resolution.[18−26] But again, it lacks the ability to characterize the detailed chemical information on surfaces. Molecular chemical structures of polymer surfaces can be detected by Fourier transform infrared spectroscopy (FTIR) and attenuated total reflection FTIR (ATR−FTIR).[32,33] The one drawback of these methods is the penetration depth of the IR beam, which is along the order of a wavelength. Therefore, ATR−FTIR detects surface layers on a micrometer scale, which lacks the surface sensitivity to elucidate surface structures/properties of materials.

Recently sum frequency generation (SFG) vibrational spectroscopy has been developed into a powerful technique to study molecular structures of surfaces in various chemical environments with a submonolayer surface sensitivity, and no vacuum is required.[34−60] SFG has been applied to study polymer surfaces, interfaces, and polymer blend surfaces.[44,45,48,49,55−60] SFG collects surface vibrational spectra that allow various functional groups present on the surface to be observed. Orientation information on the functional groups can be gathered by obtaining SFG spectra using different polarization combinations of the input and output beams.[61−63]

SFG has been applied to study surface structures of polystyrene (PS), poly(methyl methacrylate) (PMMA), and PS/PMMA blends with small amounts of PMMA.[44,45,48,57,64,65] SFG results indicate that the phenyl and ester methyl groups dominate the PS and PMMA surfaces, respectively.[44,48,57,64] SFG signals of the buried interface between PS and PMMA was detected in PS/PMMA blends with small amounts of PMMA.[45,65] In this paper, we will compare surface structures of a polymer blend to a similar copolymer using SFG, supplemented by AFM and contact angle goniometer. The polymer blend is a 1:1 (weight) mixture of PS and PMMA, and the copolymer is a diblock copolymer between PS and PMMA (PS-*co*-PMMA) with an equal weight amount of the two segments. The SFG research results on 1:1 PS:PMMA blend will also be compared to previously published blends with small amounts of PMMA to understand how different bulk ratios of polymer components

* To whom all correspondence should be addressed. E-mail: zhanc@umich.edu Fax: 734-647-4865.

10.1021/jp045647a CCC: $30.25 © 2005 American Chemical Society
Published on Web 03/12/2005

affect surface structures. PS and PMMA are two immiscible polymers that exhibit bulk phase separation and the demixing can extend to the surface due to the fact that neither polymer is able to wet the other.[18,19] Surface structures of the PS/PMMA blend and PS-*co*-PMMA have been extensively studied using various techniques. Research shows that for the polymer blend, the bulk concentration of two components controls the surface morphology. Other factors, such as solvents,[18,20] sample thickness, and chain end goups[12] can also affect polymer blend morphology. Here, we demonstrate that the copolymer surface structure and morphology is identical before and after annealing, while in the 1:1 blend, PS segregates more to the surface after annealing, and the surface becomes flatter. We also compare surface property differences of the blend and the copolymer by monitoring the time-dependent fibrinogen structural changes adsorbed on the blend and copolymer surfaces.

2. Experiment

2.1. Sample Preparation. The PS, PMMA, and PS-*co*-PMMA (with 1:1 weight ratio) were purchased from Sigma Aldrich and were used as received. Polymer films were prepared by spin-coating 2 wt % pure polymer, polymer blend (with 1:1 weight ratio), or copolymer toluene solution onto a fused silica substrate (1 in. diameter and $^1/_8$ in. thickness from ESCO products, Inc.). The samples were spun at 3000 rpm for 30 s using a spin-coater purchased from Specialty Coating System. For annealing studies the spin cast films were annealed at 125 °C for 48 h.

The fibrinogen solution with a concentration of 1 mg/mL was prepared by dissolving bovine fibrinogen in phosphate buffer (pH 7.4). Bovine fibrinogen was purchased from Sigma.

2.2. SFG Measurements. SFG is a process in which two input beams at frequencies ω_1 and ω_2 mix in a medium and generate an output beam at the sum frequency $\omega = \omega_1 + \omega_2$.[34−60] Usually ω_1 is in the visible range, and ω_2 is a tunable infrared beam. If ω_2 is scanned over the vibrational resonances of molecules, the SFG signal is resonantly enhanced, producing a vibrational spectrum characteristic of the material. The intensity of SFG spectra is related to the average orientation and orientation distribution of functional groups inside the optical field. As a second-order nonlinear optical process, SFG spectral intensity will be zero in a medium with inversion symmetry under the electric-dipole approximation. SFG spectra can be detected from the material where the inversion symmetry is broken. Most bulk materials have inversion symmetry, thus they do not generate SFG signals. At surfaces or interfaces, where inversion symmetry is necessarily broken, SFG is allowed and can therefore be used as an effective surface/interface probe. Both experimental results and theoretical calculations indicate that SFG is submonolayer sensitive for simple surfaces and interfaces. From SFG, orientation and orientation distribution of surface or interfacial functional groups can be deduced by the absolute SFG spectral intensity and the intensity ratio of SFG spectra collected using different polarization combinations of input and output laser beams.

The SFG experimental setup used in this study has been described in previous publications.[56−59] Briefly, our setup collects SFG spectra generated by overlapping a visible and tunable IR beam on the polymer surface both spatially and temporally. Both the 532 nm visible and the frequency tunable IR (650−4300 cm^{-1}) beams are 20 ps pulsed beams with a repetition rate of 20 Hz. They overlap on the surface at incident angles of 60 and 54° respectively to the surface normal with a spot diameter of 0.5 mm. The SFG spectra can be collected using a PMT with a gated integrator.

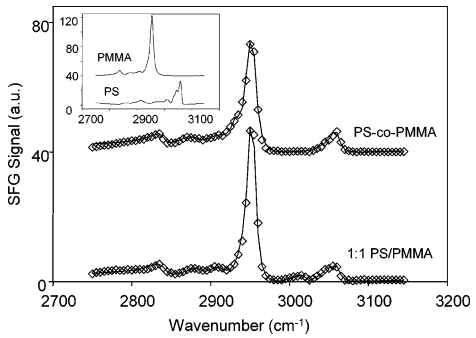

Figure 1. SFG spectra (ssp) collected from the 1:1 PS/PMMA blend and the PS-*co*-PMMA surface in the C−H stretching range before annealing. For comparison, SFG spectra collected from pure PS and pure PMMA surface are shown in the inset.

2.3. AFM. Topographic images were obtained using a PicoSPM atomic force microscope purchased from Molecular Imaging, Inc. Measurements were performed in tapping mode using cantilevers fabricated with Si_3N_4. Their average resonant frequency was 55 kHz with a spring constant of 2.8 N/m.

2.4. Contact-Angle Measurements. Contact angles (θ_a) of water on polymer films were measured at room temperature using a Cam 100 optical contact angle meter from KSV Instruments Ltd. A Hamilton syringe with a blunt tip needle was used to deliver water to the film surface. The reported values of θ_a are an average of 15 measurements taken within 30 s of applying each drop of water. Four different areas on the polymer film surface were measured.

3. Results and Discussion

3.1. SFG Results and Contact Angle Measurements on Polymer—Air Interface Before Annealing. Surface structures of pure polymers PS and PMMA have been studied in detail using SFG before.[44,48,57,64] In air, the PS surface is dominated by the phenyl groups, and such phenyl groups like to stand up on the surface. Therefore, the ssp SFG spectrum collected from PS surface in air is dominated by the ν_2 vibrational mode at ∼3060 cm^{-1}. The PMMA surface is dominated by the ester methyl groups, with such groups oriented toward the surface normal in air. The ssp SFG spectrum collected from the PMMA surface is dominated by a very strong peak at ∼2955 cm^{-1}, which is assigned to the ester methyl symmetric stretch.[57]

Figure 1 displays SFG spectra we collected from the 1:1 PS/PMMA blend and the PS-*co*-PMMA surfaces before annealing the samples. For comparison, SFG spectra collected from pure PMMA and pure PS are shown in the inset in Figure 1. For both the blend and the copolymer, there are two strong peaks in each spectrum, at ∼2955 and ∼3060 cm^{-1}, respectively. The peak at ∼2955 cm^{-1} is due to the ester methyl groups of PMMA, and the peak at ∼3060 cm^{-1} is due to the phenyl groups of PS, showing that both the blend and the copolymer surfaces are covered by both PS and PMMA components. On the copolymer surface, the intensity ratio between the ester methyl group peak at ∼2955 cm^{-1} and the phenyl group peak at ∼3060 cm^{-1} is smaller than that on the blend surface, showing that the surface coverage of PMMA might be larger on the blend surface. On the blend surface, a small peak was detected at ∼3015 cm^{-1}, which can be due to the asymmetric stretch of the ester methyl group, showing that ester methyl groups may tilt more toward the surface than those on the copolymer surface.

The SFG spectra of the 1:1 blend and copolymer have been fitted quantitatively. The fitting results shown in Table 1 also correlate well with above qualitative discussion. The fitting

TABLE 1: Fitting Results for the SFG Spectra Shown in Figure 1 and Figure 4[a]

wavenumber (cm^{-1})	blend	copolymer	blend annealed	copolymer annealed
2840 ± 1	1.0	0.8	0.3	1.0
2883 ± 2	0.4	0.4	0	0.1
2910 ± 4	0.5	0.7	0.1	0.2
2933 ± 5	0.2	0.3	0.2	0.9
2947	0	1.4	0.1	1.4
2954 ± 1	49.0	26.5	32.1	26.5
2965	0	0	0	0.7
2991 ± 1	0.4	0	0	0
3004	0	0	0	0
3010	0	0	0.3	0
3018	1.2	0	0.3	0
3030 ± 3	0.6	0	1.0	0
3047 ± 2	0.6	0	1.4	0.2
3059	4.0	5.9	9.9	5.9

[a] Results are the square of the ratio between the strength and damping factor $[(A/\Gamma)^2]$

results show that the intensity of the ~2955 cm^{-1} peak is stronger on the 1:1 blend surface, and the intensity of the ~3060 cm^{-1} phenyl peak is weaker indicating the higher coverage of PMMA on the blend surface. The fitting results also indicate that ester methyl groups may tilt more toward the surface on the blend surface.

Surface structures of PS/PMMA blends with small amounts of PMMA in the system have been investigated using SFG.[45,65] Research results indicated that SFG spectra can be collected from the PMMA at the PMMA/PS buried interfaces. For such SFG signals, the vibrational peak of the symmetric stretch of ester methyl groups has a red shift of about eight wavenumbers. Our quantitative fitting results shown in Table 1 indicate that a small peak at 2947 cm^{-1} exists in the spectra collected from both the copolymer and the 1:1 blend surface, but the intensity of this peak on the blend surface is extremely small and can be ignored. The small shoulder of the 2947 cm^{-1} on the copolymer surface may be due to the ordered structure of PMMA near the surface (e.g., the second layer), or perhaps it is due to the Fermi resonance of the surface C−H groups. The intensity of this peak on the copolymer surface is still quite small, and will not be discussed in detail in this paper. Nevertheless, we believe that the peaks in the SFG spectra collected from our blend and copolymer samples are mainly contributed by the PMMA and PS at the polymer/air interface, not from buried polymer/polymer interfaces. Therefore, we will only consider the contribution to SFG signals from the polymer blend and copolymer surface in air in this article.

Different models of domain structures for the 1:1 PS/PMMA blend have been proposed according to the results obtained from XPS and AFM studies (Figure 2).[14,25,31] The model shown in Figure 2a indicates that a layer of PMMA covers the PS after spin-coating.[14,31] The model in Figure 2b shows that separate domains of PMMA and PS exist in the entire bulk of the blend.[25,31] If the model displayed in Figure 2a is correct, we would detect SFG signal from PMMA at the buried PS/PMMA interface. As mentioned, such SFG signals should shift to the lower wavenumbers.[65] However, we did not observe such a peak shift when we compared the SFG spectra collected from the PS/PMMA blend to those of the pure PMMA surface. We believe that the real situation of our PS/PMMA blend sample is close to the model shown in Figure 2b, where no buried SFG signal can be observed.

We believe the different results of the current study and those revealed by Liu and Messmer[65] is due to the different bulk

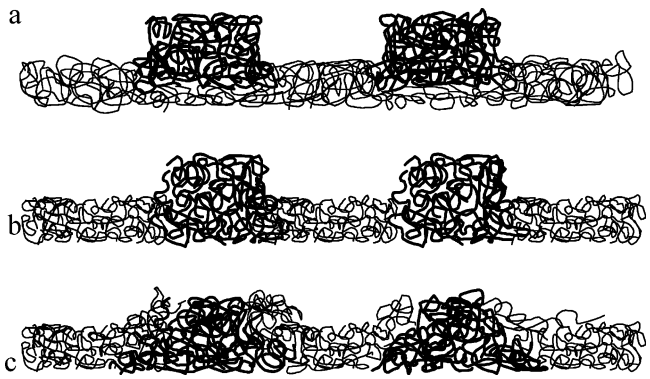

Figure 2. Models of structures of PS/PMMA blends. Thin lines represent PS, thick lines represent PMMA: (a) the model with buried PMMA/PS interface; (b) the model with no buried interface; (c) the model for the blend after annealing.

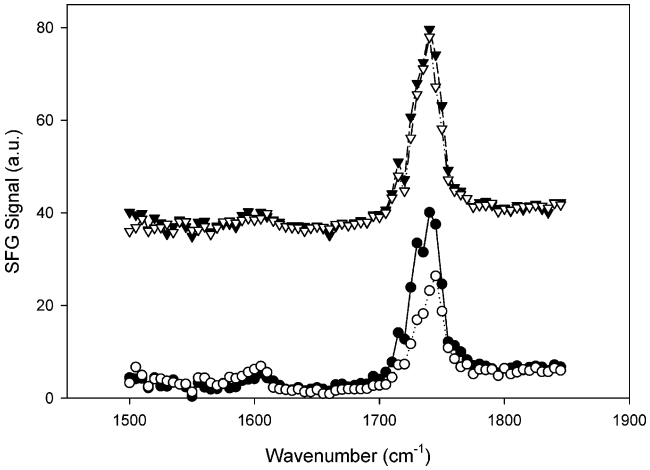

Figure 3. SFG spectra collected from the 1:1 PS/PMMA blend and the PS-*co*-PMMA surface in the C═O stretching frequency range before and after annealing. Key: upper spectra, copolymer; lower spectra, blend; black dots, before annealing; open dots, after annealing.

concentrations of PMMA in the blend from the system we are investigating. For our 1:1 PS/PMMA blend, PMMA can form separate domains in the entire bulk, from the blend/air interface to the blend/substrate interface. For the blends with small PMMA bulk concentrations studied by Liu and Messmer, PMMA is not enough to form such large domains from the substrate to the air, thus buried PS/PMMA interfaces parallel to the blend/air interface do exist in the sample, which can generate SFG signals in the ssp spectra, as detected by Liu and Messmer.

In addition to the SFG spectra collected in the C−H stretching frequency range between 2750 to 3120 cm^{-1}, we also collected SFG spectra in the C═O stretching range (Figure 3). Both C═O signals were detected from the PS/PMMA blend and the PS-*co*-PMMA surfaces, confirming that PMMA covers part of the blend and copolymer surfaces.

We measured contact angles on both the 1:1 PS/PMMA blend and the PS-*co*-PMMA blend surfaces (Table 2). For both samples before annealing, the water contact angles on the two surfaces are between the values measured on the pure PMMA and pure PS, showing that the surfaces are covered by both components. The water contact angle on the 1:1 blend surface is similar to that on the PS-*co*-PMMA surface, showing that the two surfaces have similar hydrophobicity. This is attributed to the combination effect of coverage and orientation of functional groups on the two surfaces.

TABLE 2: Water Contact Angles Measured on the PS, PMMA, PS-*co*-PMMA, and 1:1 PS/PMMA Blend Surfaces[a]

	$(\theta_a)°$	
polymer	CA (H_2O)	anneal CA (H_2O)
PS	88.8	88.5
PMMA	67.9	68.0
PS-*co*-PMMA	72.7	72.6
1:1 PS/PMMA	72.9	78.5

[a] The error bar of each measurement is approximately 0.5 deg.

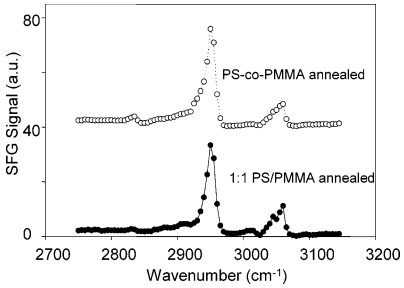

Figure 4. SFG spectra collected from the 1:1 PS/PMMA blend and the PS-*co*-PMMA surface in the C−H stretching range after annealing.

3.2. Annealing Effects. In the previous section, we have studied surfaces of the 1:1 PS/PMMA blend and the PS-*co*-PMMA using SFG and contact angle measurements. Our research indicated that on both the blend surface and the copolymer surface, both PMMA and PS components exist. Since PS has a lower surface energy than that of PMMA, from a surface energy point of view, at the equilibrium, it should segregate to the surface and cover the entire surface. However, the surface energy effect might be balanced by the entropy factor and therefore some PMMA may appear on the surface even at the equilibrium state. In addition, our sample preparation procedures may result in nonequilibrium surface structures of the blend and copolymer.

In this research, samples were made by spin-coating. Since the solubility of PMMA and PS are different in the solvent toluene, during the spin-coating process, the solvent evaporated very quickly, leaving the polymer samples in a nonequilibrated state. One method to prepare these polymer blend and copolymer samples in equilibrium is to anneal these samples at higher temperatures. Here we want to monitor the surface structural changes of the PS/PMMA blend and the PS-*co*-PMMA after annealing. We found that the 1:1 PS/PMMA and the PS-*co*-PMMA have drastic differences in surface structural responses to annealing.

We believe that if a nonequilibrium effect exists, it can be reversed by heating the polymer films at an elevated temperature above the glass transition temperatures (T_g) of both PS and PMMA, which are 100 and 106 °C, respectively. Therefore, we annealed samples at 125 °C for 48 h. We collected SFG spectra and measured water contact angles of both blend and copolymer surfaces after annealing. SFG spectra are shown in Figure 4, and the contact angles are listed in Table 2.

To our surprise, both SFG results and contact angle measurements indicate that the copolymer surfaces have no structural change. Figure 4 shows that the SFG spectrum collected from the PS-*co*-PMMA surface after annealing overlaps with that collected from the same sample before annealing quite well in the C−H stretching frequency range. Both the intensity ratio and the absolute intensity of the symmetric stretch of ester methyl groups and phenyl groups are the same in the spectra. Quantitative fitting results for both SFG spectra are listed in Table 1 and confirm that the two spectra are very similar. Figure 3 indicates that the C═O stretching signals of PMMA on the PS-*co*-PMMA surface before and after annealing are also quite similar, showing that the C═O groups of PMMA adopt the same surface structure before and after annealing.

We also measured the water contact angle on the PS-*co*-PMMA surface after annealing the sample (Table 2). As in the SFG spectra, the contact angle is the same as that measured on the surface before annealing. Both SFG studies and contact angle measurements show that there is no surface structural change of PS-*co*-PMMA upon annealing. The PS-*co*-PMMA surface structure may reach the equilibrated state even before annealing.

The annealing effect on the 1:1 PS/PMMA blend surface has been investigated using AFM and XPS before.[14] Research results indicate that after annealing, low surface energy component PS segregates more to the surface, while the PMMA surface coverage drops. Our SFG and contact angle measurement results are compatible with these previous studies. The SFG studies and contact angle measurements on the 1:1 PS/PMMA blend show markedly different results compared to those of the copolymer we reported above. Figure 4 shows that the SFG spectrum collected from the blend surface after annealing is different from that before the annealing (shown in Figure 1): The SFG signal of the ∼2955 cm^{-1} symmetric stretch of ester methyl groups decreases and the ∼3060 cm^{-1} phenyl group signal increases. The change of SFG signal intensity in the SFG spectrum might be due to the coverage, orientation, and orientational distribution of surface functional groups. We believe that the signal intensity changes here indicate the increase of surface coverage of phenyl groups and the reduction of surface coverage of ester methyl groups, which agrees with the hypothesis that the more low surface energy component PS should segregate to the surface when the equilibrium is reached. Quantitative spectral fitting (Table 1) of the SFG spectra collected from the 1:1 blend surface before and after annealing confirms the above qualitative discussion.

Figure 3 also shows that after annealing, the SFG C═O signal collected from the 1:1 blend surface decreases, indicating the lower surface coverage of C═O groups on the surface. This also confirms that the surface coverage of PMMA on the blend surface reduces after annealing, which correlates well to the SFG results in the C−H stretching frequency range.

The contact angle measurements confirm again that the surface coverage of PS increases on the surface. Table 2 shows that the water contact angle markedly increased after annealing, proving that the surface is more hydrophobic after annealing.

From our SFG studies and contact angle measurements described above, we can see markedly different surface structural responses for the PS/PMMA blend and PS-*co*-PMMA copolymer to annealing. This can be explained by the different mobility of different components in the polymer blend and copolymer. In the polymer blend, PS and PMMA are physically mixed; therefore, they have the freedom to move around. Upon annealing, the low surface energy component PS can move to the surface, resulting in a higher surface coverage of PS molecules. In the copolymer, two blocks of PMMA and PS are covalently bound together. When a copolymer molecule moves to the surface, both PS and PMMA blocks move to the surface. Therefore, if we consider a copolymer molecule as a whole, the surface segregation of one component such as the blend case will not occur. Of course, upon annealing, reorientation of surface copolymer molecules to expose more PS segments to the surface may occur, but was not detected in our system. Our results show that the surface structure of PS-*co*-PMMA is very stable, and will not change upon annealing above the glass

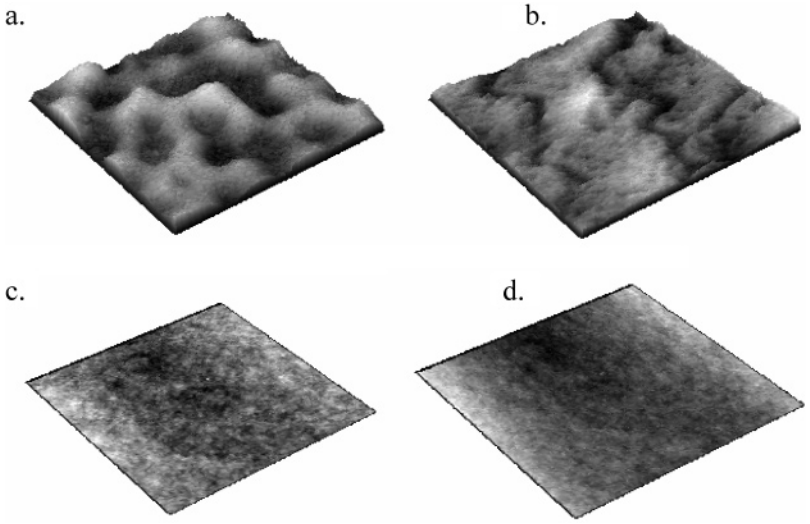

Figure 5. AFM images of the 1:1 PS/PMMA blend and the PS-*co*-PMMA surfaces before and after annealing: (a) blend before annealing; (b) blend after annealing; (c) copolymer before annealing; (d) copolymer after annealing. All images are 2 μm by 2 μm images.

transition temperatures of both components. On the contrary, the PS/PMMA blend surface has more PS coverage after annealing. Since no buried PMMA signal was observed, the ordered interface between PS and PMMA was not formed during the annealing process. A schematic plot is shown in Figure 2c regarding the annealing effect on the PS/PMMA blend surface. As shown in Figure 2c, no ordered buried interface was formed after annealing.

3.3. AFM Studies. As mentioned, PS/PMMA blend surfaces have been extensively studied by AFM.[14,25] Research shows that the 1:1 PS/PMMA surface is not flat. Here we want to compare the surface morphology of the copolymer and the 1:1 blend and discuss the surface roughness effect on SFG and contact angle measurements.

We imaged the surfaces of the 1:1 PS/PMMA film and PS-*co*-PMMA copolymer before and after annealing using AFM (Figure 5). Figure 5 shows that the PS-*co*-PMMA surface is flat before and after annealing, the root-mean-square roughness in a 2 μm by 2 μm area is much smaller than 0.5 nm for both cases. Therefore, previously discussed SFG and contact angle measurement results are obtained from flat surfaces. The possible complication of surface roughness on our previous data analysis for the PS-*co*-PMMA surfaces does not need to be considered.

As revealed in the literature,[14] AFM topographic images we observed in the experiment show that the 1:1 PS/PMMA surface is quite rough before annealing, with a root-mean-square roughness of $\sim$5 nm in a 2 μm by 2 μm area. After annealing, the surface becomes flatter, with a root-mean-square roughness of $\sim$3 nm in the same area. The surface is still rougher than the PS-*co*-PMMA surface we investigated here. The roughness of the PS/PMMA blend surface may complicate our previous SFG and contact angle analysis. However, we believe that both ester methyl and phenyl groups must have very broad orientation distributions on the polymer blend as well as copolymer surfaces; thus, the conclusion of above qualitative discussions on SFG results will not be affected by the different surface roughness of various samples. In particular, from Figure 5, we can see that the surface height varies gradually. Our quantitative data fitting was used to confirm our qualitative discussion, rather than deduce the quantitative surface structure; thus, we believe that the conclusion will not be affected by such a surface roughness. Also, we believe that the roughness in the nanometer scale will not substantially influence the contact angle measurement results.

3.4. Protein Adsorption Behavior. From our SFG, AFM, and contact angle measurement studies, we elucidated the surface structural differences between the 1:1 PS/PMMA blend and the PS-*co*-PMMA. In addition, the annealing effect on surface structures has been examined. In this section, we hope to show the different surface properties of the blend and copolymer by investigating their protein adsorption behaviors.

Polymer materials, including pure polymers, polymer blends, and copolymers are extensively applied as biomedical materials.[1−4] The biocompatibility of a polymer material can be inferred by studying the protein adsorption on this polymer. The first body reaction after a polymer is implanted is protein adsorption. The adsorbed proteins will determine later body reactions and finally determine whether the material will be accepted or rejected by the body. Surface chemical structures as well as surface morphology can mediate protein adsorption behavior. Here, we will study fibrinogen adsorption on PS/PMMA blend and copolymer surfaces.

Fibrinogen ($\sim$340 kDa) is a large protein that is the major substrate of thrombin and the major protein in clot formation. As a fibrinogen molecule adsorbs on a polymer surface, it undergoes structural, conformational, or orientational changes. Such changes greatly affect the binding capability of fibrinogen molecules to platelets. The surface-bound fibrinogen has an important role in thrombus formation.[66−69] Therefore, understanding the molecular structures of fibrinogen molecules adsorbed on different surfaces should contribute to the understanding of platelet adhesion on such surfaces and thus the blood compatibility of these materials. The amide I signal is a good indicator of the secondary structure of fibrinogen. We demonstrated for the first time that it is feasible to detect SFG amide I signals from interfacial proteins.[70] In this study, we will adopt the total reflection geometry to detect SFG amide signals at the blend/fibrinogen solution and the copolymer/fibrinogen solution interfaces to compare how different PS/PMMA blend and the PS-*co*-PMMA surfaces mediate adsorbed fibrinogen structures. Figure 6 shows the SFG amide signal collected from the PS/fibrinogen interface. The spectral features of SFG amide signals collected from fibrinogen after initial adsorption on PMMA, the blend, and the copolymer are not very different from that shown in Figure 6. Instead of examining the detailed

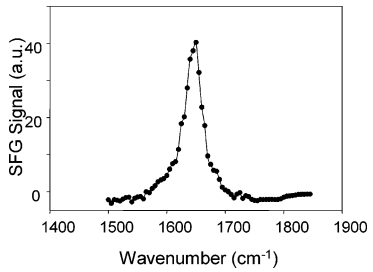

Figure 6. SFG spectrum collected from the PS/fibrinogen solution interface.

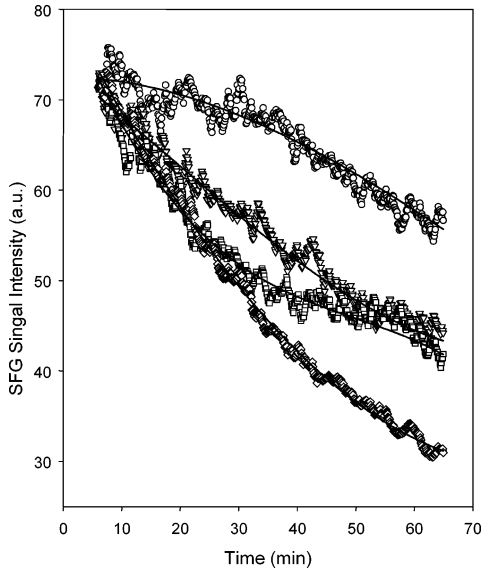

Figure 7. Time-dependent SFG amide signal intensity collected from fibrinogen at interfaces between fibrinogen solution and pure PMMA, pure PS, PS/PMMA blend and PS-*co*-PMMA before annealing. Dots are experimental data, and lines are fitted results. Curves from the top to the bottom are as follows: PS, PS-*co*-PMMA, PS/PMMA blend, PMMA.

fibrinogen structures on the blend and copolymer surfaces by quantitatively analyzing the SFG amide signals, which is under our current study and will be published elsewhere, here we want to demonstrate that different PS/PMMA blend and the PS-*co*-PMMA copolymer surfaces can affect fibrinogen adsorption differently by observing time-dependent SFG signal intensity changes.

We monitored the SFG signal's intensity change by collecting the SFG signal with the infrared frequency fixed at the amide I peak center around 1650 cm^{-1}. The peak at about 1650 cm^{-1} is contributed by the α-helical structure in the fibrinogen. The collected intensity changes as a function of time, indicating fibrinogen structural/orientational changes after adsorbed onto different surfaces. The time-dependent SFG amide signal intensities detected from pure PS, pure PMMA, 1:1 PS/PMMA and PS-*co*-PMMA before annealing are shown in Figure 7. For comparison, we normalized the initial spectral intensity on various polymer materials to the same intensity. Figure 7 shows that, on the PS surface, the intensity changes only slightly after more than 65 min, showing that the fibrinogen structure only slightly changes after adsorbed on the PS surface during this period of time. On the contrary, the intensity decreases substantially on the pure PMMA surface, showing that fibrinogen structure has significant changes within 65 min. The time-dependent behavior of fibrinogen amide intensity at the PS-*co*-PMMA interface is intermediate to the PMMA surface and the PS surface. The intensity dropped more substantially than that on the PS surface, but less substantially than that on the PMMA surface. We believe that the copolymer surface does not have separated PS and PMMA domains, the two components are mixed together on the surface. Therefore, when fibrinogen molecules interact with the copolymer surface, they experience the average property of the PMMA and the PS surface.

The first part of the time dependent changes of fibrinogen adsorbed on the 1:1PS/PMMA blend surface is much similar to that on the PMMA surface, but after a while, the spectral intensity change is similar to that on the PS surface. The fact that PS/PMMA showed a different profile after 30 min may be because of the surface domain structures. In the first 30 min, the signal change is dominated by contributions from fibrinogen molecules adsorbed on the PMMA domains. Later, when the signals of fibrinogen on the PMMA domain surfaces decrease substantially, the spectral changes of fibrinogen on the PS domain surfaces dominate the overall trend. The overall time-dependent change is again intermediate to that on the PMMA and the PS surface, but different from that on the copolymer surface. As we mentioned, before annealing, the surface coverage of PMMA on the blend is higher than that on the copolymer surface. Therefore, the overall time dependent change of fibrinogen on the blend surface is more similar to the PMMA surface than the copolymer surface is, especially in the first 30 min. The fibrinogen adsorption experiments here demonstrate that the surface structure differences of the PS/PMMA blend and copolymer induce their different surface properties, inducing different time-dependent structural/orientational changes of adsorbed proteins.

4. Conclusion

In this research, through SFG, contact angle measurement, AFM, and protein adsorption studies, we elucidated surface structure and properties of a 1:1 PS/PMMA blend and a copolymer PS-*co*-PMMA with the same amount of PS and PMMA in the system. We demonstrated that surface structures and properties of the blend and the copolymer are quite different. Both PS and PMMA components were detected on the blend and the copolymer surfaces. For the polymer blend, PMMA and PS segregate into domains on the surface as well as in the entire bulk. No ordered buried interfaces between PMMA and PS were detected. After annealing, the blend surface becomes flatter, with more PS segregated to the surface. The surface structure and surface free energy are the same before and after annealing on the PS-*co*-PMMA surface. No domain structure was detected on the copolymer surface. Our SFG C−H and C═O signals and the contact angle measurements correlated with each other quite well. Fibrinogen adsorption studies indicate that surface properties of both the blend and the copolymer are intermediate to the two pure components. The different time-dependent structural/orientational changes of fibrinogen adsorbed on the blend and copolymer surfaces show the different surface structures of the blend and the copolymer. Such a change on the blend surface is more similar to that on the PMMA surface, which is correlated well to the SFG study on the blend surface which shows more surface coverage of PMMA on the blend surface.

Acknowledgment. This work is supported by the National Science Foundation (Grant No. 0315857) and the start-up funds from the University of Michigan. William C. Johnson wants to thank the Rackham Graduate School for the RMF fellowship.

References and Notes

(1) Ratner, B. D.; Castner, D. G. *Surface Modification of Polymeric Biomaterials*; Plenum Press: New York, 1996.

(2) Feast, W. J.; Munro, H. S. *Polymer Surfaces and Interfaces I*; John Wiley and Sons: New York, 1987.
(3) Feast, W. J.; Munro, H. S.; Richards, R. W. *Polymer Surfaces and Interfaces II*; John Wiley and Sons: New York, 1992.
(4) Park, J. B.; Lakes, R. S. *Biomaterials: An Introduction*; Plenum Press: New York, 1992.
(5) Richards, R. W.; Peace, S. K. *Polymer Surfaces and Interfaces III*; John Wiley and Sons: Chichester, U.K., 1999.
(6) Garbassi, F.; Morra, M.; Occhiello, E. *Polymer Surfaces: From Physics to Technology*, revised and updated ed.; John Wiley and Sons: Chichester, U.K., 1998.
(7) Andrade, J. D. *Polymer Surface Dynamics*; Plenum Press: New York, 1988.
(8) Tanaka, K.; Takahara, A.; Tisato, K. *Macromolecules* **1998**, *31*, 863−869.
(9) Restos, H.; Margiolaki, A.; Messaritaki, A.; Anastasiadis, S. H. *Macromolecules* **2001**, *34*, 5295−5305.
(10) Kajiyama, T.; Tanaka, K.; Ge, S. R.; Takahara, A. *Prog. Surf. Sci.* **1996**, *52*, 1.
(11) Chen, C.; Wang, J.; Woodcock, S. E.; Chen, Z. *Langmuir* **2002**, *18*, 1302−1309.
(12) Kajiyama, T.; Tanaka, K.; Takahara, A. *Macromolecules* **1998**, *31*, 3746−3749.
(13) Artyushkova, K.; Wall, B.; Koenig, J.; Fulghum, J. E. *Appl. Spectrosc.* **2000**, *54*, 1549−1558.
(14) Ton-That, C.; Shard, A. G.; Daley, R.; Bradley, R. H. *Macromolecules* **2000**, *33*, 8453−8459.
(15) Affrossman, S.; Kiff, T.; O'Neil, S. A.; Pethrick, R. A.; Richards, R. W. *Macromolecules* **1999**, *32*, 2721−2730.
(16) Feng, J. Y.; Weng, L. T.; Li, F.; Chan, C. M. *Surf. Interface Anal.* **2000**, *29*, 168−174.
(17) Vanden Eynde, X.; Bertrand, P. *Appl. Surf. Sci.* **1999**, *141*, 1−20.
(18) Walheim, S.; Boltau, M.; Mlynek, J.; Krausch, G.; Steiner, U.; *Macromolecules* **1997**, *30*, 4995−5003.
(19) Qu, S.; Clarke, C. J.; Liu, Y.; Rafailovich, M. H.; Sokolov, J.; Phelan, K. C.; Krausch, G. *Macromolecules* **1997**, *30*, 3640−3645.
(20) Kumacheva, E.; Li, L.; Winnik, M. A.; Shinozaki, D. M.; Cheng, P. C. *Langmuir* **1997**, *13*, 2483−2489.
(21) Takahara, A.; Nakamura, K.; Tanaka, K.; Kajiyama, T. *Macromol. Symp.* **2000**, *159*, 89−96.
(22) Grandy, D. B.; Hourston, D. J.; Price, D. M.; Reading, M.; Silva, G. C.; Song, M.; Sykes, P. A. *Macromolecules* **2000**, *33*, 9348−9359.
(23) Affrossman, S.; Henn, G.; O'Neil, S. A.; Pethrick, R. A.; Stamm, M. *Macromolecules* **1996**, *29*, 5010−5016.
(24) Slep, D.; Asselta, J.; Rafailovish, M. H.; Sokolov, J.; Winesett, D. A.; Smith, A. P.; Ade, H.; Strzhemechny, Y.; Schwarz, S. A. Sauer, B. S. *Langmuir* **1998**, *14*, 4860−4864.
(25) Tanaka, K.; Takahara, A.; Kajiyama, T. *Macromolecules* **1996**, *29*, 3232−3239.
(26) Dalnoki-Veress, K.; Forrest, J. A.; Dutcher, J. R. *Phys. Rev. E* **1998**, *57*, 5811−5817.
(27) Muller-Buschbaum, P.; Gutmann, J. S.; Stamm, M. *Macromolecules* **2000**, *33*, 4886−4895.
(28) Grull, H.; Schreyer, A.; Berk, N. F.; Majkrzak, C. F.; Han, C. C. *Europhys. Lett.* **2000**, *50*, 107−112.
(29) Wu, S. *Polymer Interfaces and Adhesion*; Marcel Dekker: New York, 1982.
(30) Balkenende, A. R.; van de Boogaard, H. J. A. P.; Scholten, M.; Willard, N. P. *Langmuir* **1998**, *14*, 5907−5912.
(31) Ton-That, C.; Shard, A. G.; Teare, D. O. H.; Bradley, R. H. *Polymer* **2001**, *42*, 1121−1129.
(32) Wang, D.; Ji, J.; Feng, L. X. *Macromolecules* **2000**, *33*, 8472−8478.
(33) Cheng, S. S.; Chittur, K. K.; Sukenik, S. N.; Culp, L. A.; Lewandowska, K. J. *Colloid Interface Sci.* **1994**, *162*, 135−143.
(34) Shen, Y. R. *The Principles of Nonlinear Optics*; Wiley: New York, 1984.
(35) Shen, Y. R. *Annu. Rev. Phys. Chem.* **1989**, *40*, 327−350.
(36) Miranda, P. B.; Shen, Y. R. *J. Phys. Chem. B* **1999**, *103*, 3292−3307.
(37) Bain, C. D. *J. Chem. Soc., Faraday Trans.* **1995**, *91*, 1281−1296.
(38) Chen, Z.; Gracias, D. H.; Somarjai, G. A. *Appl. Phys. B: Laser Opt.* **1999**, *68*, 549−557.
(39) Gracias, D. H.; Chen, Z.; Shen, Y. R.; Somarjai, G. A. *Acc. Chem. Res.* **1999**, *320*, 930−940.
(40) Schultz, M. J.; Schnitzer, C.; Simonelli, D.; Baldelli, S. *Int. Rev. Phys. Chem.* **2000**, *19*, 123−153.
(41) Eisenthal, K. B. *Chem. Rev.* **1996**, *96*, 1343−1360.
(42) Scatena, L. F.; Brown, M. G.; Richmond, G. L. *Science* **2001**, *292*, 908−912.
(43) Ye, S.; Noda, H.; Morita, S.; Uosaki, K.; Osawa, M. *Langmuir* **2003**, *19*, 2238−2242.
(44) Briggman, K. A.; Stephenson, J. C.; Wallace, W. E.; Richter, L. J. *J. Phys. Chem. B* **2001**, *105*, 2785−2791.
(45) Liu, Y.; Messmer, M. C. *J. Am. Chem. Soc.* **2002**, *124*, 9714−9715.
(46) Kim, J.; Cremer, P. S. *J. Am. Chem. Soc.* **2000**, *122*, 12371−12372.
(47) Jung, S. Y.; Lim, S. M.; Albertorio, F.; Kim, G.; Gurau, M. C.; Yang, R. D.; Holden, M. A.; Cremer, P. S. *J. Am. Chem. Soc.* **2003**, *125*, 12782−12786.
(48) Gautman, K. S.; Scwab, A. D.; Dhinojwala, A.; Zhang, D.; Dougai, S. M.; Yeganeh, M. S. *Phys. Rev. Lett.* **2000**, *85*, 3854−3857.
(49) Harp, G. P.; Gautam, K. S.; Dhinojwala, A. *J. Am. Chem. Soc.* **2002**, *124*, 7908−7909.
(50) Ma, G.; Allen, H. C. *J. Am. Chem. Soc.* **2002**, *124*, 9374−9375.
(51) Moad, A. J.; Simpson, G. J. *J. Phys. Chem. B* **2004**, *108*, 3548−3562.
(52) Liu, J.; Conboy, J. C. *J. Am. Chem. Soc.* **2004**, *126*, 8376−8377.
(53) Konek, C. T.; Musorrafiti, M. J.; Al-Abadleh, H. A.; Bertin, P. A.; Nguyen, S. T.; Geiger, F. M. *J. Am. Chem. Soc.*, ASAP article.
(54) Rivera-Rubero, S.; Baldelli, S. *J. Am. Chem. Soc.*, ASAP article.
(55) Miyamae, T.; Yamada, Y.; Uyama, H.; Nozoye, H. *Appl. Surf. Sci.* **2001**, *180*, 126−137.
(56) Wang, J.; Woodcock, S. E.; Buck, S. M.; Chen, C. Y.; Chen, Z. *J. Am. Chem. Soc.*, **2001**, *123*, 9470−9471.
(57) Wang, J.; Chen, C. Y.; Buck, S. M.; Chen, Z. *J. Phys. Chem. B* **2001**, *105*, 12118−12125.
(58) Wang, J.; Paszti, Z.; Even, M. A.; Chen, Z. *J. Am. Chem. Soc.* **2002**, *124*, 7016−7023.
(59) Chen, C. Y.; Wang, J.; Even, M. A.; Chen, Z. *Macromolecules* **2003**, *36*, 4478−4484.
(60) Chen, Z.; Shen, Y. R.; Somorjai, G. A. *Annu. Rev. Phys. Chem.* **2002**, *53*, 437−465.
(61) Zhuang, X.; Miranda, P. B.; Kim, D.; Shen, Y. R. *Phys. Rev. B* **1999**, *59*, 12633−12640.
(62) Hirose, C.; Yamamoto, H.; Akamatsu, N.; Domen, K. J. *J. Phys. Chem.* **1993**, *97*, 10064−10069.
(63) Hirose, C.; Akamatsu, N.; Domen, K. *Appl. Spectrosc.* **1992**, *46*, 1051−1072.
(64) Zhang, D.; Dougal, S. M.; Yeganeh, M. S. *Langmuir* **2000**, *16*, 4528−4532.
(65) Liu, Y.; Messmer, M. C. *J. Phys. Chem. B* **2003**, *107*, 9774−9779.
(66) Pitt, W. G.; Park, K.; Cooper, S. L. *J. Colloid Interface Sci.* **1986**, *111*, 343−362.
(67) Lindon, J. N.; McManama, G.; Kushner, L.; Merrill, E. W.; Salzman, E. W. *Blood* **1986**, *68*, 355−362.
(68) Pekala, R. W.; Merrill, E. W.; Lindon, J.; Kushner, L.; Salzman, E. W. *Biomaterials* **1986**, *7*, 379−385.
(69) Balasubramanian, V.; Grusin, N. K.; Bucher, R. W.; Turitto, V. T.; Slack, S. M. *J. Biomed. Mater. Res.* **1999**, *44*, 253−260.
(70) Wang, J.; Even, M. A.; Chen, X.; Schmaier, A. H.; Waite, J. H.; Chen, Z. *J. Am. Chem. Soc.* 2003, *125*, 9914−9915.